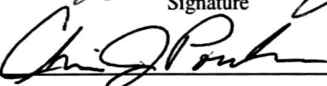**Aislinn E. Deely**

Photon dose affects dissolved organic matter apparent quantum yields in Alaskan Arctic surface waters
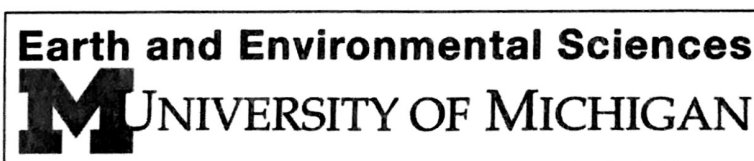
submitted in partial fulfillment of the requirements for the degree of
Master of Science in Earth and Environmental Sciences
Department of Earth and Environmental Sciences
The University of Michigan

Accepted by:

Signature	Name	Date
(signature)	Nathan Sheldon	9 April 2018
(signature)	Rose Cory	9 April 2018
(Department Chair Signature)	Chris Poulsen	April 11, 2018

Earth and Environmental Sciences
UNIVERSITY OF MICHIGAN

Photon dose affects dissolved organic matter apparent quantum yields in Alaskan Arctic surface waters

Aislinn E. Deely

Abstract

Photochemical, or light-driven, processing of dissolved organic matter (DOM) in inland waters can completely degrade DOM to carbon dioxide (CO_2), a greenhouse gas, through photo-mineralization or partially degrade DOM through partial photo-oxidation. Evidence suggests that the lability of DOM, quantified as an apparent quantum yield (AQY, ϕ_λ), is not constant with increasing light exposure. Thus, the rate of photochemical processing is not constant during light exposure in sunlit surface waters as DOM ϕ_λ changes. Findings in this study show that $\phi_{PM,\lambda}$ (photo-mineralization) typically decreases as photon dose increases, while $\phi_{PPO,\lambda}$ (partial photo-oxidation) does not show a consistent trend. Differences in DOM chemistry between sites and dates sampled are likely controlling differences in $\phi_{PM,\lambda}$ and $\phi_{PPO,\lambda}$ trends with increasing photon dose. Daily areal rates of photo-mineralization calculated with $\phi_{PM,\lambda}$ after a low photon dose are an overestimate by a factor of 2.08 ± 0.18 compared to rates calculated with $\phi_{PM,\lambda}$ from a higher photon dose, while daily areal rates of partial photo-oxidation calculated with $\phi_{PPO,\lambda}$ after a low photon dose are an overestimate by a factor of 1.15 ± 0.10 compared to rates calculated with $\phi_{PPO,\lambda}$ from a higher photon dose. Because partial photo-oxidation $\phi_{PPO,\lambda}$ does not show a consistent trend with increasing photon dose, the impact of low vs. high photon dose experimentally determined $\phi_{PPO,\lambda}$ on calculated areal rates is not as large as the impact of $\phi_{PM,\lambda}$. Understanding how photon dose and DOM chemistry control the photochemical degradation of DOM will further constrain current estimates of how much CO_2 and partially-oxidized DOM is produced through photochemical processes in these arctic surface waters.

Introduction

Inland waters transport large amounts of carbon from land to the atmosphere and to the ocean, similar in magnitude to the net flux of carbon between land and the atmosphere (Cole et al. 2007). Much of the carbon in inland waters is in the form of dissolved organic matter (DOM). DOM is a heterogeneous mixture of organic molecules, resulting from the breakdown of bacterial and plant organic matter. DOM has multiple fates as it moves through inland waters: (1) DOM is stored in sediments and the hyporheic zone, (2) DOM is converted to carbon dioxide (CO_2, a greenhouse gas) in the water column by photochemical reactions and microbial respiration, which can then be emitted to the atmosphere, or (3) DOM is partially oxidized by photochemical reactions, which can be respired by microbes or transported to the ocean (Battin et al. 2009; Cole et al. 2007; Wetzel 2001; Cory et al. 2013, 2014). This DOM fate is particularly important in the Arctic, where permafrost soils contain twice as much carbon as there is currently in the atmosphere (Tarnocai et al. 2009). Permafrost soils are thawing and releasing carbon to inland waters in the Arctic (Zhang et al. 2006; Keller et al. 2010). Understanding the controls on DOM fate, and how this could change as carbon is released from permafrost soils, is vital for inland water, and thus, global carbon budgets.

Previous work suggests that the relative balance of DOM completely converted to CO_2 by light vs. partially oxidized by light may vary due to differences in prior light exposure that DOM has received during transit in arctic surface waters (Cory et al. 2013, 2014). DOM with little prior light exposure (e.g., exported from soils) is easily converted to CO_2 by light (Cory et al. 2013, 2014), thus this DOM is labile to photochemical processing. As water travels downstream and total photon dose increases, the fraction of DOM readily converted to CO_2 by light may be depleted. As these labile fractions are removed, partial photo-oxidation becomes the dominant

fate of DOM (Cory et al. 2014*).* However, changes in DOM lability to photochemical processes, or how easily the DOM is processed by light, with increasing photon dose are poorly understood.

Studies have shown that the rate of photochemical CO_2 production in seawater is not constant with increasing light exposure (Farjalla et al. 2001; Lindell et al. 2000; Miles and Brezonik 1981; Miller and Zepp 1995; Powers and Miller 2015a, 2015b). Miller and Zepp (1995) suggested that the greater production of CO_2 in short light exposure experiments compared to long light exposure experiments indicated the presence of a DOM pool that was very labile to photo-mineralization. Farjalla et al. (2001) observed nonlinear CO_2 production with increased light exposure, however they attributed it to photobleaching, where colored DOM (CDOM) is degraded to uncolored DOM thus reducing the rate of light absorption (Wetzel et al. 1995; Miller and Zepp 1995; Pullin et al. 2004). Powers and Miller (2015a, 2015b) showed that initial rates of CO_2 production were faster than during longer exposures, and that photobleaching did not account for the nonlinear production. However, the sites, light exposure times, and light source are not consistent across the studies described above, and therefore it is difficult to determine a common control on photo-mineralization with increasing light exposure. Additionally, these studies did not calculate apparent quantum yields (AQYs, ϕ_λ), which is a measure of DOM lability quantified as mol CO_2 produced per mol photons absorbed by CDOM for photo-mineralization ($\phi_{PM,\lambda}$), normalizing the photochemically produced CO_2 to the rate of light absorption, which is not constant across sites (Vahatalo et al. 2000; Hu et al. 2002). Photo-mineralization with increasing light exposure has not yet been investigated in freshwaters.

Molecular oxygen (O_2) is consumed in waters when light absorbed by CDOM initiates the production of reactive intermediates and radicals, called reactive oxygen species (ROS) (Miles and Brezonik 1981). However, few studies have measured photochemical O_2 consumption with

increasing photon dose (Amon and Benner 1996; Andrews et al. 2000; Lindell et al. 2000; Miles and Brezonik 1981). Amon and Benner (1996) observed a decrease in the rate of O_2 consumption with increasing light exposure, however absorbance was not measured, therefore it cannot be concluded that the observed decrease in O_2 consumption was due to changes in DOM lability rather than photobleaching. Miles and Brezonik (1981) observed rapid O_2 consumption rates initially, and then slower rates at longer light exposure times. Only one study has quantified changes in DOM ϕ for photo-oxidation ($\phi_{PO,\lambda}$) (Andrews et al. 2000). ϕ_{PO} decreased with increasing absorbed light dose in seawater and was suggested to be due to fractions within the DOM pool having different photo-labilities (Andrews et al. 2000). Investigating O_2 consumption, in addition to CO_2 production, with increasing light exposure is not well understood.

ROS, such as hydrogen peroxide (H_2O_2), hydroxyl radical ($\bullet OH$), and singlet oxygen ($^1O_2$), generated through oxygen consumption have multiple fates in waters (Cooper and Zika 1983; Mopper and Zhou 1990; Latch and McNeill 2006). One fate of ROS is to oxidize DOM to CO_2 or partially oxidized DOM (Cory et al. 2010a). ROS can also be quenched by DOM exhibiting anti-oxidant properties, ultimately suppressing or slowing down photo-oxidation (Blough and Zepp 1995; Aeschbacher et al. 2012). However, anti-oxidant DOM can be degraded by light, reducing the amount of ROS that are quenched with increasing photon dose. With increasing photon dose, ϕ_λ for $\bullet OH$ and H_2O_2 decrease while ϕ_λ for $^1O_2$ increase, likely due to the degradation of DOM with anti-oxidant properties (Sharpless et al. 2014). Thus, photo-oxidation by ROS is controlled by changes in ϕ_λ for ROS and quenching of ROS by anti-oxidant DOM.

Previous work has shown that aquatic DOM has a higher electron donating capacity (EDC) than terrestrial DOM and microbial DOM, and thus has a higher anti-oxidant capacity (Aeschbacher et al. 2012). EDCs of DOM correlated with titrated phenol contents, suggesting that

phenolic moieties contain major electron donating groups (Aeschbacher et al. 2012). Irreversible oxidation of DOM in the environment results in a depletion of electron donating phenolic moieties (Aeschbacher et al. 2012). Upon exposure to light, DOM exhibits a decrease in average molecular weight, a loss of aromatic groups, and more specifically, the disappearance of lignin phenols (Aeschbacher et al. 2012; Sharpless et al. 2014). There is also a positive relationship between EDC and $SUVA_{254}$, a proxy for aromaticity of DOM (Sharpless et al. 2014). DOM exhibits a larger absolute loss in absorbance in the UV range (280-400 nm), however there is a greater % loss of absorbance in the visible range (400-700 nm), leading to an increase in the DOM anti-oxidant capacity proxy E2/E3, which is the ratio of absorbance coefficients at 254 nm to 365 nm (Sharpless et al. 2014). The increase in E2/E3 and decrease in EDC with increasing light exposure suggest that DOM with anti-oxidant properties are being destroyed due to photo-degradation (Sharpless et al. 2014). Therefore, the initial composition of DOM controls anti-oxidant capacity, where high anti-oxidant capacity DOM would be expected to have a high average molecular weight, high aromaticity, and low E2/E3.

The initial composition of DOM and effect of increasing photon dose on DOM ϕ_λ could change throughout the growing season in the Arctic, the period of time each year when the tundra thaws and vegetation can grow (May through August). In the Arctic, the spring thaw delivers a large pulse of DOM to surface waters (Townsend-Small et al. 2010) that may not have been previously exposed to light. As time passes from the spring thaw, DOM present in freshwaters is increasingly exposed to light as residence time increases during low flow conditions (Cory et al. 2014, 2015). Additionally, increasing soil thaw depth throughout the season could influence DOM composition and ϕ_λ. Ward and Cory 2016 determined that there were trends in ϕ_λ dependent on soil depth. $\phi_{PM,350}$ was similar between shallower and deeper organic matter (Ward and Cory

2016). However, $\phi_{PPO,350}$ was greater in DOM leached from deeper organic matter (Ward and Cory 2016). The study suggested that this greater $\phi_{PPO,350}$ was due to deeper organic matter having a lower phenolic content than shallower organic matter, thus decreasing the DOM anti-oxidant capacity and allowing for more DOM to be partially-oxidized. Ward and Cory 2015 determined that there were trends in DOM chemistry leached from soils of different depths in a watershed in the Alaskan Arctic. With increasing soil depth, slope ratio (S_R, inverse relationship with average molecular weight) increased, $SUVA_{254}$ decreased, and fluorescence index (FI, proxy for DOM source) increased (Ward and Cory 2015). This indicates that the initial composition of deeper organic matter had a lower average molecular weight, aromaticity, and originated from a different source. Seasonal light exposure and these changes in ϕ_λ and DOM chemistry with soil depth could influence the effect of photon dose on ϕ_λ, as thaw depth increases between May and August in the Arctic.

Photochemical processes of DOM in inland waters are an important component of the arctic carbon budget (Cory et al. 2014). Light converts a substantial amount of DOM to CO_2 in arctic surface waters through photo-mineralization, accounting for 55% of the CO_2 released to the atmosphere in the Kuparuk River basin (Cory et al. 2014). In this basin, 45% of DOM degradation was due to partial photo-oxidation (Cory et al. 2014). Changes in DOM $\phi_{PM,\lambda}$, $\phi_{PPO,\lambda}$, and areal rates of photochemical processes with increasing photon dose have not yet been incorporated in to current estimates of photo-mineralization and partial photo-oxidation rates in these arctic surface waters.

Changes in DOM ϕ_λ have been studied in seawater from various sites, however this has not been investigated in freshwaters or in the Arctic, where photochemistry largely contributes to carbon budgets. Previous studies have cautioned that using short exposure experiments to quantify

ϕ_λ would lead to an overestimation of areal rates or that using longer exposure experiments would lead to underestimation of areal ratess (Andrews et al. 2000; Powers and Miller 2015b). Changes in $\phi_{PPO,\lambda}$ with increasing photon dose have never been quantified. The objective of this study was to investigate changes in DOM $\phi_{PM,\lambda}$ and $\phi_{PPO,\lambda}$ with increasing photon dose, and the impact of ϕ_λ on calculated daily areal rates of photochemical processes. This study also examined changes in ϕ_λ with increasing photon dose relative to initial DOM composition and the influence of anti-oxidants at different sites and times throughout the arctic growing season. This study addressed these knowledge gaps by testing the effect of photon dose on well-characterized and representative freshwaters in the Arctic, and exposed surface waters to increasing photon doses to be able to compare the effect of photon dose on changes in ϕ_λ between different waters (where DOM composition and ϕ_λ are known to be different).

Methods

Site Descriptions

Surface water was collected from two rivers and two streams (characterized in Table 1) on the North Slope of Alaska in May through July 2017. These streams and rivers drain some organic and mineral soils, underlain by permafrost (Osterkamp and Payne 1981; McNamara et al. 1998). Maximum annual thaw depth on the North Slope is less than 1.0 m (Carter et al. 1987). ϕ_λ and areal rates of photochemical processes have previously been quantified and calculated for these sites (Cory et al. 2013, 2014, 2015). (1) Imnavait Creek is a beaded headwater stream (1st order) running through a glacial valley (2.2 km^2; Kane et al. 1989) formed during the Sagavanirktok glaciation (~250 ka) in the Kuparuk River basin (Hamilton 1986). The vegetation is primarily tussock cottongrass and the soil is classified as moist acidic tundra (Ward and Cory 2016).

Imnavait Creek has a high DOC concentration and a pH of 5-6 (Cory et al. 2014). (2) Toolik Inlet is the inlet stream (3rd order) of Toolik Lake, the site of the Arctic Long-Term Ecological Research (LTER) project, draining a watershed that contains several lakes (46.6 km^2; Kling et al. 2000). Glacial till from the Itkillik I glaciation (50-100 ka) is found on ridges in the watershed and stream valleys contain glacial till and outwash deposits from the Itkillik II glaciation (10-25 ka; Hamilton and Porter 1975). The vegetation present is typically upland tussock, riparian birch and willow and the soil is classified as wet sedge tundra (Keller et al. 2010). Toolik Inlet has an intermediate DOC concentration and circumneutral pH (Cory et al. 2014). (3) The Kuparuk River (4th order) originates in the foothills of the Brooks Range and flows to the Arctic Ocean, draining an area of about 8000 km^2, which contains lakes (Hershey et al. 1997; McGuire et al. 2009). The river is on deposits from ~250 ka. The Kuparuk River has an intermediate DOC concentration and circumneutral pH (Cory et al. 2014). The vegetation present is tussock cottongrass, and riparian dwarf willows and birches and the soil is classified as wet sedge tundra (Hershey et al. 1997). (4) The Sagavanirktok River is the second largest river on the North Slope (> 4th order), draining an area of about 15,000 km^2, which contains lakes (McGuire et al. 2009; Levine and Whalen 2001; Cory et al. 2014). The river is on surfaces deposited during the Itkillik I and II glaciations (Hobara et al. 2013). The Sagavanirktok River has a low DOC concentration and a pH of ~8 (Cory et al. 2014). The vegetation present is riparian shrubs, and willows and the soil is classified as wet sedge tundra (Giblin et al. 1994).

Sample Collection and Water Chemistry

Surface water was collected from streams and rivers from a depth of 0.1 m, in high density polyethylene bottles, pre-rinsed with stream water three times. Temperature, conductivity, and pH

were measured in the field. Filtered (pre-combusted Whatman GF/F) subsamples taken for dissolved organic carbon concentration (DOC) were acidified with trace-metal grade hydrochloric acid to approximately pH 3 and stored in the dark at 4°C until analysis using a high-temperature platinum-catalyzed combustion followed by infrared detection of CO_2 (Shimadzu TOC-V).

Photochemical Oxidation Experiments

Surface water samples were 0.22 μm filtered (sterile Sterivex) in to high density polyethylene bottles using a peristaltic pump (Geotech Geopump) and kept in the dark at room temperature to equilibrate with the atmosphere overnight. Filtered water was placed in gas-tight, pre-combusted 12 mL borosilicate exetainer vials (Labco Inc.) without headspace, and exposed to natural light at Toolik Field Station (68°38' N, 149°36' W). Exposure times and corresponding photon doses are provided in Table 2. Due to high background DIC and low CDOM absorbance in the Sagavanirktok River waters, and thus a lower rate of light absorption, photon doses received were about double the doses for the three other sites. However, even though the water received higher photon doses, the Sagavanirktok River did not have a higher light absorbed by CDOM compared to the other three sites. Each exposure time consisted of four light exposed replicates alongside four aluminum foil wrapped dark control replicates for each analysis (dissolved O_2 (DO), dissolved inorganic carbon (DIC), and CDOM/fluorescent DOM (FDOM)). Ambient temperatures during exposure ranged from 1 to 25 °C; May and June experiments were exposed at low temperatures and July experiments were exposed during higher temperatures. Light exposed waters reached a higher temperature during the experiments, relative to the dark controls. However, due to the low activation energies of photochemical reactions, there is a weak temperature dependence on the rates (Schwarzenbach et al. 2003). Total irradiance measurements were taken every five minutes during the experiments (Yankee Environmental Systems, Inc. UVA-

1 (280-320 nm) and UVB-1 (320-400 nm); Li-Cor, Quantum Model LI-190SB for PAR (400-700 nm)). At the end of each exposure time, sample replicates for DO and DIC were killed with $HgCl_2$ (added at 1% volume of the exetainer vial). All replicates were refrigerated in the dark until analysis.

Photochemical O_2 consumption was quantified as the change in DO relative to dark controls using membrane inlet mass spectrometry (MIMS) as previously described (Cory et al. 2010a). Photochemical production of CO_2 was quantified as the change in DIC measured relative to dark controls using a DIC analyzer (Apollo SciTech, Inc.). Excitation Emission Matrices (EEMs) and absorbance for CDOM/FDOM were measured using a spectrofluorometer (Horiba Aqualog) in a 1-cm quartz cuvette in reference to a Milli-Q blank. Data presented in this study are an average of four independent light reps, each relative to an independent dark rep, plus or minus standard error.

Apparent Quantum Yield Calculations

Apparent quantum yields (AQY, ϕ_λ) quantify the lability of DOM to photochemical processes. ϕ_λ normalizes the measured O_2 consumption or CO_2 production to the rate of light absorption, in terms of moles of O_2 consumed or moles of CO_2 produced per moles of photons absorbed by CDOM for photo-oxidation and photo-mineralization, respectively (Vähätalo et al. 2000).

The apparent quantum yield spectrum is assumed to decrease exponentially with increasing wavelength (Johannessen et al. 2001), as shown in Equation 1:

$$\phi_\lambda = c \, e^{-d\lambda} \tag{1}$$

where c (mol C mol^{-1} photons) and d (nm^{-1}) are positive parameters calculated using an unconstrained nonlinear optimization in Matlab.

$Q_{a,\lambda}$ is the light absorbed by the water in the exetainer vial, calculated using Equation 2:

$$Q_{a\lambda}\ (mol\ photons\ m^{-2}\ d^{-1}) = Q_{dso-\lambda}(1 - e^{-K_{d\lambda}z}) \tag{2}$$

Where $Q_{dso-,\lambda}$ is the spectrum of light just below the water surface (mol photons m^{-2} d^{-1}), $K_{d,\lambda}$ is the light extinction coefficient (m^{-1}), and z is pathlength of the borosilicate exetainers (m). These calculations take photobleaching throughout the light exposure experiment into account (Miller and Zepp 1995).

Direct measurements of natural light at Toolik Field Station were apportioned to a "clear sky" modeled solar spectrum generated with the NREL Simple Model of Atmospheric Radiation Transfer (SMARTS). The modeled solar spectrum in the UV-Visible range was generated and normalized using parameters previously described for Toolik Field Station (Cory et al. 2014). This spectrum was then separated into direct and diffuse components. A turbidity correction was quantified as a daily average cloudiness factor (F) as the ratio of mean measured to mean modeled (SMARTS) solar irradiance at Toolik Field Station. F varied from ~0.6 on cloudy days to ~1 for clear sky days during these light exposure experiments. Turbidity scatter, assumed to be independent of wavelength, was applied to all wavelengths. Wavelength dependent Rayleigh scattering was calculated following Bird and Riordan (1986). The angle of incidence for diffuse radiation was set to 45° and the angle of incidence for direct radiation was calculated from the local zenith angle at 1-hour intervals (NREL Solar Position Calculator). Radiative transfer below the water surface in the experiment exetainer was calculated separately for the direct and diffuse photon fluxes as previously described (Cory et al. 2014).

The rate of photochemical oxidation is the product of three spectra (Equation 3): the

apparent quantum yield, the irradiance reaching the water column, and the spectrum of light absorbed by CDOM.

$$\textit{Photochemical oxidation (mmol } O_2 \textit{ or } CO_2 \textit{ } m^{-2} \textit{ } d^{-1}) = \int_{\lambda_{min}}^{\lambda_{max}} \phi_\lambda Q_{a\lambda} \frac{aCDOM_\lambda}{atot_\lambda} d\lambda \quad (3)$$

Where λ_{min} and λ_{max} are the minimum and maximum wavelengths of light contributing to the photo-oxidation of DOM (280 and 700 nm, respectively), ϕ_λ is the apparent quantum yield for photo-oxidation or photo-mineralization, $a_{CDOM,\lambda}$ is the Naperian absorption coefficient of CDOM (m^{-1}), and $a_{tot,,\lambda}$ is the total light absorption in the water column (CDOM, particles and water; m^{-1}). In these experiments, CDOM is assumed to be the only light absorbing constituent in these filtered waters, therefore the ratio of $a_{CDOM,\lambda}$ to $a_{tot,,\lambda}$ is 1.

To quantify the lability of DOM over the entire course of each light exposure, ϕ_λ were determined by setting the total measured reactant (O_2) on the left side of Equation 3 and used the measured photons absorbed by CDOM (using $Q_{a,\lambda}$ and $a_{CDOM,\lambda}$) in the exetainer vials during the total light exposure to solve for ϕ_λ after each photon dose. These equations were also used to determine the ϕ_λ for photo-mineralization using the measured product (CO_2). For each photon dose, the O_2 consumed and the CO_2 produced were calculated relative to dark controls.

To quantify the lability of DOM that was degraded by light in between increases in photon dose, the ϕ_λ were also calculated incrementally. These photochemical experiments each consisted of five photon doses (Table 2), where t_1 received the lowest photon dose and t_5 received the highest photon dose in each experiment. For t_1, photobleaching, O_2 consumed, CO_2 produced, and $Q_{dso-,\lambda}$ relative to dark controls were used to determine ϕ_λ, quantifying the lability of the DOM that was degraded by light during the lowest photon dose. Then for t_2, photobleaching, the O_2 consumed, the CO_2 produced, and $Q_{dso-,\lambda}$ relative to t_1 were used to determine ϕ_λ. Therefore, the ϕ_λ calculated for t_2 quantifies the lability of the DOM that was degraded by light only between t_1 and t_2. For t_3,

photobleaching, the O_2 consumed, the CO_2 produced, and $Q_{dso-\lambda}$ relative to t_2 were used to determine ϕ_λ, thereby quantifying the DOM that was degraded by light only between t_2 and t_3. The same methods were used to calculate ϕ_λ for t_4 and t_5 in these experiments. Thus, with these incremental ϕ_λ, we can assess changes in DOM lability during increases in photon dose.

Partial photo-oxidation is calculated using two assumptions: (1) 1 mole of O_2 is consumed to produce 1 mole of CO_2 in photo-mineralization and (2) 0.5 mole of O_2 that is in excess of the 1:1 stoichiometry is consumed to oxidize 1 mole of carbon (Andrews et al. 2000). Partial photo-oxidation AQYs are calculated using Equation 4:

$$\phi_{PPO,350} \left(\tfrac{\text{mmol } C_{ox}}{\text{mol photons}}\right) = \left(\phi_{PO,350} - \left(\phi_{PM,350}\right)\left(\tfrac{1 \text{ mol } O_2 \text{ consumed}}{1 \text{ mol } CO_2 \text{ produced}}\right)\right)\left(\tfrac{1 \text{ mol } C \text{ oxidized}}{0.5 \text{ mol } O_2 \text{ consumed}}\right) \quad (4)$$

Where $\phi_{PPO,350}$ is the partial photo-oxidation ϕ_λ at 350 nm, $\phi_{PO,350}$ is the photo-oxidation ϕ_λ at 350 nm, and $\phi_{PM,350}$ is the photo-mineralization ϕ_λ at 350 nm. The $\phi_{PM,350}$ and $\phi_{PO,350}$ for both the entire photon dose and the incremental photon doses were used to calculate $\phi_{PPO,350}$, quantifying $\phi_{PPO,350}$ over the entire photon dose and in increments of light exposure. $\phi_{PM,350}$ (mmol CO_2 produced mol photons^{-1}) and $\phi_{PPO,350}$ (mmol C_{ox} mol photons^{-1}) presented in this study are an average of four reps plus or minus standard error.

Photochemical Areal Rate Calculations

Daily areal rates of photochemical processes were calculated using Equation 3, with the experimentally determined ϕ_λ for each photon dose, the measured attenuation coefficient of the surface water, and direct measurements of natural light at Toolik Field Station for a 24-hour period. Areal rate calculations for Imnavait Creek, Toolik Inlet, and the Kuparuk River assumed that CDOM was the main light absorbing constituent in the water column, thus $a_{CDOM,\lambda}/a_{tot,\lambda} = 1$. For

the Sagavanirktok River areal rate calculations, a $a_{CDOM,\lambda}/a_{tot,\lambda}$ factor of 0.15 was used. The Sagavanirktok River was turbid on the sample collection dates in June and July 2017, and thus were similar conditions to those described in Cory et al. (2013). Areal rates were calculated using the light spectra for 5-June-2017 to 6-June-2017 (May and June experiments), 7-July-2017 to 8-July-2017 (early July experiments), and 27-July-2017 to 28-July-2017 (late July experiments). Each areal rate calculation began at 6:00 on the first day and ran to 6:00 on the next day. A time weighted F factor was used in these calculations (75% first day, 25% second day). The rates were calculated using an average water depth of 0.5 m.

A single daily areal rate was also calculated using the incremental ϕ_λ, factoring in changes in ϕ_λ with increasing light exposure, as well as changing the absorption spectra after each increment of light exposure to incorporate photobleaching into the areal rate calculation. These calculations were done using the same light spectra as listed above. Each ϕ_λ was used to calculate an areal rate in increments corresponding to its order during the light exposure experiment: t_1 (6:00 – 8:00), t_2 (8:00 – 10:00), t_3 (10:00 – 14:00), t_4 (14:00 – 18:00), and t_5 (18:00 – 6:00 the following day). The areal rates calculated in each of these increments were then summed up to receive a daily areal rate.

Results

Initial Chemistry

Initial water chemistry is provided in Table 3. Surface waters samples from Imnavait Creek had a pH ranging 4.8 ± 0.1 to 5.9 ± 0.1, temperatures ranged 0.1 to 16°C, and conductivity ranged 11 to 13 µs cm^{-1} on dates sampled. In Toolik Inlet, pH ranged 7.3 ± 0.1 to 7.6 ± 0.1, temperatures ranged 0.1 to 12°C, and conductivity ranged 85 to 92 µs cm^{-1} on dates sampled. For the Kuparuk

River, pH ranged 6.7 ± 0.1 to 7.8 ± 0.1, temperatures ranged 0.1 to 10°C, and conductivity ranged 18 to 77 µs cm^{-1} on dates sampled. In the Sagavanirktok River, pH ranged 7.8 ± 0.1 to 8.1± 0.1, temperatures ranged 5 to 11°C, and conductivity ranged 189 to 245 µs cm^{-1} on dates sampled. Initial DOM chemistry is provided in Table 3. Highest DOC concentrations and CDOM absorbance were in May/June surface water samples. DOC content, absorbance, aromaticity, and optical proxies varied by site and date.

Initial DOM chemistry differs by site and date (Figures 1, 2). There is no difference in S_R between May and July in Imnavait Creek, Toolik Inlet, and the Kuparuk River. Slope ratio (S_R), the ratio of slopes of the absorbance spectra at 275-295 nm: 300-350 nm, is an optical proxy that is inversely related to average molecular weight (Helms et al. 2008). In the Sagavanirktok River, S_R is greater in June than in July. E2/E3 is the ratio of absorbance at 254:365 nm, and has an inverse relationship with EDC, thus a higher E2/E3 indicates a low anti-oxidant capacity (Sharpless et al. 2014). A higher E2/E3 is observed in July for Imnavait Creek, Toolik Inlet, and the Kuparuk River. The Sagavanirktok River shows no difference in E2/E3 between June and July. SUVA$_{254}$, the DOC normalized decadic absorption coefficient at 254 nm, is a proxy for DOM aromaticity (Weishaar et al. 2003). Imnavait has a higher SUVA$_{254}$ in July, Toolik Inlet shows no change, and the Kuparuk River and the Sagavanirktok River have a higher SUVA$_{254}$ in May and June. Fluorescence Index (FI) is a proxy for DOM source and aromatic carbon, calculated from the ratio of emission intensities at excitation = 370 nm emission at 470:520 nm (Cory et al. 2010b). C/A is the ratio of EEM emission peaks at 350-540 nm to 250:450 nm, which are related to humic DOM (Coble et al. 1996). In all sites, there is a higher FI and C/A in July.

Effect of increasing photon dose on $\phi_{PM,350}$

In May and June, $\phi_{PM,350}$ decreased with increasing photon dose for all waters tested (Figure 3). In early July, $\phi_{PM,350}$ decreased with increasing photon dose for Imnavait Creek and the Kuparuk River, the only waters tested on this date (Figure 4). In late July, $\phi_{PM,350}$ decreased with increasing photon dose for Toolik Inlet water, but increased or remained the same with increasing photon dose in the other three waters tested (Figure 5).

Effect of increasing photon dose on $\phi_{PPO,350}$

The effect of photon dose on $\phi_{PPO,350}$ differed by date and by stream or river (Figures 6-8). With increasing photon dose, Imnavait Creek DOM $\phi_{PPO,350}$ decreased in May, early July, and late July. Toolik Inlet DOM $\phi_{PPO,350}$ showed no change in May and decreased in July with increasing light exposure. Kuparuk River DOM $\phi_{PPO,350}$ increased in May and early July, but $\phi_{PPO,350}$ decreased in late July, with increasing photon dose. Sagavanirktok River DOM $\phi_{PPO,350}$ increased in June but remained the same in July with increasing photon dose.

$\phi_{PM,350}$ and $\phi_{PPO,350}$ through the season

In Figure 9, many points fall above the 1:1 line, suggesting that $\phi_{PM,350}$ is higher in July vs. May or June. However, sometimes in the Kuparuk River and the Sagavanirktok River, May and June $\phi_{PM,350}$ is higher or, for all sites, sometimes there is no difference observed. In general, $\phi_{PPO,350}$ is greater in July vs. May or June (Figure 9). In the Kuparuk River and the Sagavanirktok River, $\phi_{PPO,350}$ is higher in July compared to May and June, and this is also observed sometimes in Imnavait Creek and Toolik Inlet. Toolik Inlet $\phi_{PPO,350}$ is sometimes higher in May, and in both Imnavait Creek and Toolik Inlet, there is sometimes no change.

Discussion

DOM composition is different between sites

There were differences in DOM composition between sites and dates sampled. Only the Sagavanirktok River shows a seasonal change in S_R and is the only site to not show a seasonal difference in E2/E3. In Imnavait Creek, Toolik Inlet, and the Kuparuk River, the average molecular weight does not change between May and July, but the DOM anti-oxidant capacity decreases at these three sites. SUVA$_{254}$ trends varied by site, indicating that Imnavait Creek had a higher aromaticity in July, Toolik Inlet had the same aromaticity in July, and the Kuparuk River and the Sagavanirktok River had a lower aromaticity in July. Fluorescence Index and C/A were higher in July across all sites, indicating that the source and composition of the DOM at all sites changed between May/June and July. These CDOM and FDOM properties indicate that DOM source and composition differs by sites and date.

The Sagavanirktok River DOM composition was different from the other sites. Between June and July, Sagavanirktok River DOM showed an increase in average molecular weight, a decrease in aromaticity, and maintained its anti-oxidant capacity. The Sagavanirktok River also demonstrated the greatest change in DOM source by an 8.7 ± 0.4 % increase in FI in July (Figure 2). These observations indicate that the DOM found in the Sagavanirktok River watershed is substantially different from the DOM in the watersheds of Imnavait Creek, Toolik Inlet, and the Kuparuk River.

DOM photo-lability with increasing photon dose differs by site, date, and process.

Most cumulative $\phi_{PM,350}$ align with observations and predictions in the literature that $\phi_{PM,350}$ decreased with increasing photon dose. In May, June, and early July experiments, as photon dose

increased, $\phi_{PM,350}$ decreased and then plateaued. In late July, Toolik Inlet $\phi_{PM,350}$ decreased with increasing photon dose, while $\phi_{PM,350}$ in the three other sites increased or stayed the same. Decreases in $\phi_{PM,350}$ with increasing photon dose could be attributed to photo-mineralization removing labile DOM from the DOM pool, leaving behind a pool that is less labile to photo-mineralization.

Changes in $\phi_{PPO,350}$ are not consistent between site and date. Previous work quantified a decrease in the lability of DOM to photo-oxidation with increasing light exposure (Andrews et al. 2000), thus a decrease in partial photo-oxidation lability would be expected as labile moieties are removed from the DOM pool. However, this was not observed in this study. DOM is partially-oxidized by ROS generated after CDOM absorbs light (Cooper and Zika 1983; Mopper and Zhou 1990; Latch and McNeill 2006). Previous work has shown that the ϕ_λ of different ROS do not follow the same trends with increasing light exposure. ϕ_λ for H_2O_2 and •OH production decrease with increasing light exposure, while ϕ_λ for $^1O_2$ production increase (Sharpless et al. 2014). These opposite trends in ROS production could lead to increases and decreases in $\phi_{PPO,350}$ as more $^1O_2$ is produced later in the light exposure period and less H_2O_2 and •OH is produced. Additionally, $\phi_{PPO,350}$ is influenced by DOM with anti-oxidant properties. DOM with a high anti-oxidant capacity would quench ROS and prevent partial photo-oxidation. However, DOM with anti-oxidant properties can be degraded with increasing photon dose, allowing ROS to partially oxidize more DOM at higher photon doses. Changes in ϕ of ROS, the presence of anti-oxidant DOM, and the degradation of anti-oxidant DOM could be contributing to differences in $\phi_{PPO,350}$ with increasing photon dose by site and date.

We would expect $\phi_{PM,350}$ and $\phi_{PPO,350}$ to be greater in May/June after the spring thaw, which brings large amounts of fresh DOM to arctic surface waters, than in July when low flow conditions

would increase light exposure history, thus decreasing $\phi_{PM,350}$ and $\phi_{PPO,350}$ (Townsend-Small et al. 2010, Cory et al. 2015). However, in Figure 9, $\phi_{PM,350}$ points fall on, above, and below the 1:1 line, indicating that $\phi_{PM,350}$ does not have clear seasonal differences, suggesting that there is not an effect of seasonal light exposure. In general, $\phi_{PPO,350}$ is greater in late July than in May and June, plotting above the 1:1 line in Figure 9. Later in the season, the DOM is not from the same source and does not have the same composition as the DOM from the early season spring thaw (Figures 1, 2). Thus, DOM source and composition likely control seasonal $\phi_{PM,350}$ and $\phi_{PPO,350}$ more than seasonal light exposure.

There were differences in DOM chemistry between sites and dates (Figures 1, 2). At all sites, FI is greater in late July. FI decreases with light exposure, therefore we would expect to observe a lower FI in July if seasonal light exposure was the cause for changes in $\phi_{PM,350}$ and $\phi_{PPO,350}$ with increasing photon dose. An increase in FI later in the season supports the hypothesis that DOM source has a greater impact on $\phi_{PM,350}$ and $\phi_{PPO,350}$ than seasonal light exposure. One factor that increases FI is the contribution of microbial DOM, however microbial contribution to DOM is low in arctic streams and rivers (Cory et al. 2007). Another factor that increases FI is DOM draining from a deeper soil depth (Ward and Cory 2015, Ward and Cory 2016). Thus, the increase in FI at all sites later in the season suggests that the streams and rivers are draining deeper and older organic matter with a different composition from DOM delivered during the spring thaw. Furthermore, previous work has investigated differences in $\phi_{PM,350}$ and $\phi_{PPO,350}$ between shallow and deeper organic matter in the Alaskan Arctic. Little difference in $\phi_{PM,350}$ was observed between shallow and deeper organic matter, consistent with little difference in $\phi_{PM,350}$ by season in this study. However, $\phi_{PPO,350}$ was greater for deeper organic matter than shallow organic matter. The study suggested that the shallower organic matter had a greater phenolic content, and thus a greater

anti-oxidant capacity, than the deeper organic matter. The observed FI increase in this study strongly suggests that DOM draining from deeper soil, with a lower anti-oxidant capacity, is likely leading to greater $\phi_{PPO,350}$ later in the season in these streams and rivers.

Properties of anti-oxidant capacity

Optical properties of DOM have previously been correlated with EDC, phenolic content, and anti-oxidant capacity. However, iron (Fe) has been shown to affect the absorption spectra of DOM, thus affecting $SUVA_{254}$, E2/E3 and S_R optical proxies that are calculated with absorbance intensities (Poulin et al. 2014). Fe concentrations in arctic streams and rivers are high during the spring thaw and decrease through the season (Rember and Trefry 2004). Therefore, optical proxies for water samples collected in May and June are likely affected by Fe transported to these waters during the spring thaw. Imnavait Creek maintains a high Fe concentration after the spring thaw, and thus the optical proxies for this stream in July are likely also affected by absorption of light by Fe (Page et al. 2014). Additionally, E2/E3 may not be an accurate depiction of anti-oxidant capacity during low CDOM conditions, such as in the Sagavanirktok River in July, due to variability in the absorbance spectra at longer wavelengths. These factors make it difficult to qualitatively examine anti-oxidant capacity with these proxies between sites and dates.

Optical proxies in this study did not always agree on the relative anti-oxidant capacity between sites. DOM with a high anti-oxidant capacity would be expected to have a high average molecular weight (low S_R), high aromaticity (high $SUVA_{254}$), and a low E2/E3. In May/June, Imnavait Creek had the highest molecular weight and the Kuparuk River had the highest aromaticity and lowest E2/E3; the Sagavanirktok River had the lowest molecular weight and highest E2/E3 and Toolik Inlet had the lowest aromaticity. In July, Imnavait Creek had the highest

molecular weight and aromaticity and the Sagavanirktok River had the lowest E2/E3; the Sagavanirktok River also had the lowest molecular weight and aromaticity and Toolik Inlet had the highest E2/E3. Specifically, the properties of DOM in the Sagavanirktok River in July highlight the contradiction between molecular weight and aromaticity proxies with the anti-oxidant capacity proxy.

Partial photo-oxidation lability is the best indicator of relative DOM anti-oxidant capacity. Imnavait Creek DOM has a high aromaticity, but does not have the lowest E2/E3, which is likely influenced by the presence of Fe in the water. However, Imnavait Creek consistently has low $\phi_{PPO,350}$. In this study, the Sagavanirktok River had the greatest $\phi_{PPO,350}$, indicating that the DOM in the Sagavanirktok River has little to no anti-oxidant capacity. DOM in the Sagavanirktok River is not able to fend off oxidation, and therefore $\phi_{PPO,350}$ indicates that the DOM has low anti-oxidant capacity. Using $\phi_{PPO,350}$ as a qualitative measure of anti-oxidant capacity, the Sagavanirktok River has the lowest anti-oxidant capacity, followed by the Kuparuk River and Imnavait Creek, and Toolik Inlet has the highest anti-oxidant capacity. These observations are consistent with previously published $\phi_{PPO,350}$ for these sites (Cory et al. 2014).

Effect of changing ϕ_λ on calculated daily areal rates of photochemical processes

Studies have cautioned that using ϕ_λ from longer exposure experiments would underestimate the rapid photo-oxidation or mineralization of DOM during short exposure times and others suggested that using ϕ_λ from short exposure experiments would overestimate photo-oxidation or mineralization. When calculated with each experimentally determined ϕ_λ as photon dose increases, the areal water column rate of photo-mineralization decreases (Figure 10). Previous ϕ_λ and water column areal rates of photo-mineralization and partial photo-oxidation for

the streams and rivers in this study have been determined from 12-hour exposure experiments (Cory et al. 2014). To determine the effect of photon dose on daily areal rates calculated with a single ϕ_λ spectrum, the areal rate calculated from the shortest photon dose ϕ_λ was compared to the areal rate calculated from the 12-hour exposure ϕ_λ for each site and date. On average, $\phi_{PM,\lambda}$ of the lowest photon dose yielded an areal rate of photo-mineralization that was an overestimate by a factor of 2.08 ± 0.18 compared to the rate calculated with the $\phi_{PM,\lambda}$ determined from the 12-hour exposure experiment. $\phi_{PPO,\lambda}$ of the lowest photon dose yielded an areal rate of partial photo-oxidation that was a slight overestimate by a factor of 1.15 ± 0.10 compared to the rate calculated with the $\phi_{PPO,\lambda}$ determined from the 12-hour exposure experiment. Therefore, the areal rates of both photo-mineralization and partial photo-oxidation were impacted by differences in ϕ_λ between experiments that received low or high photon doses, however the impact on the areal rate of photo-mineralization was greater than on partial photo-oxidation.

Figure 11 and Figure 12 demonstrate how the areal rate calculated with the single ϕ_λ spectra from the 12-hour experiment compares to the areal rate calculated with changing ϕ_λ and photobleaching as light exposure increases. For photo-mineralization (Figure 11), only two points (June and July Sagavanirktok River areal rates) fall on the 1:1 line, indicating that the constant $\phi_{PM,\lambda}$ areal rate was not significantly different from the changing $\phi_{PM,\lambda}$ areal rate. There are four points (May and early July Imnavait Creek, July Toolik Inlet, and May Kuparuk River areal rates) that plot slightly below the 1:1 line, indicating that the constant $\phi_{PM,\lambda}$ areal rate calculation was a slight overestimate relative to the areal rate calculated with changing $\phi_{PM,\lambda}$ and photobleaching. This could be due to the fact that the changing $\phi_{PM,\lambda}$ areal rate takes photobleaching into account. However, a recalculation of the areal rate with changing ϕ_{PM} with a constant absorption spectrum showed change only within error, indicating that photobleaching was not greatly impacting the

areal rates of photo-mineralization of DOM with the changing $\phi_{PM,\lambda}$. Thus, these waters were light-limited, because accounting for photobleaching did not significantly affect the areal rate. This observation is in line with the controls on DOM degradation discussed in Cory et al. (2015). The areal calculated with a constant $\phi_{PM,\lambda}$, being an overestimate is likely due to the areal rate calculated with a changing $\phi_{PM,\lambda}$ containing increments of low $\phi_{PM,\lambda}$, later in the exposure calculation. Four points (late July Imnavait Creek, May Toolik Inlet, and both July Kuparuk River areal rates) plot above the 1:1 line, indicating that the constant $\phi_{PM,\lambda}$, rate is an underestimate of the daily areal rate of photo-mineralization. This is likely due to the changing $\phi_{PM,\lambda}$ rate taking in to account the high initial lability of DOM at low photon doses. When comparing the areal rate calculated using the constant $\phi_{PM,\lambda}$, compared to the areal rate calculated with a changing $\phi_{PM,\lambda}$ daily photo-mineralization rates differ by a factor of 1.00 ± 0.11.

For partial photo-oxidation (Figure 12), May Imnavait Creek, May and early July Kuparuk River, and June and July Sagavanirktok River areal rates plot on the 1:1 line, indicating that the areal rate calculated with constant ϕ_{PPO}, was not significantly different from the areal rate calculated with changing $\phi_{PPO,\lambda}$. Three points (both July Imanavait Creek and July Toolik Inlet areal rates) plotted slightly above the 1:1 line, indicating that the areal rate calculated with constant $\phi_{PPO,\lambda}$ was an underestimate. Photodecarboxylation produces CO_2 without consuming O_2, therefore photodecarboxylation makes the calculation for $\phi_{PPO,\lambda}$ conservative. Leached organic matter from the Imnavait watershed has previously been show to undergo photodecarboxylation (Ward and Cory 2016). Additionally, the Toolik Inlet experiment exhibited photodecarboxylation in one of the light exposure increments. Therefore, photodecarboxylation that is accounted for throughout the areal rate calculated with constant $\phi_{PPO,\lambda}$ could be making the areal rate conservative, while the changing $\phi_{PPO,\lambda}$ calculation only accounts for photodecarboxylation in

some increments of light exposure if photodecarboxylation was not happening during the entire length of the experiment. Two points (May Toolik Inlet and late July Kuparuk River areal rates) plot below the 1:1 line, indicating that the constant $\phi_{PPO,\lambda}$ areal rate of partial photo-oxidation is an overestimate. A recalculation of the areal rate with changing $\phi_{PPO,\lambda}$ using a constant absorption spectrum showed change within error, thus photobleaching was not causing the overestimate in the areal rate calculated with constant $\phi_{PPO,\lambda}$. In these two experiments, there were periods of no detectable partial photo-oxidation, as observed in the incremental $\phi_{PPO,\lambda}$ Therefore, the rate calculated with constant $\phi_{PPO,\lambda}$ is accounting for constant partial photo-oxidation, leading it to be greater in magnitude than the rate calculated with changing $\phi_{PPO,\lambda}$. When comparing the areal rate calculated using the 12-hour light exposure $\phi_{PPO,\lambda}$ compared to the areal rate calculated with a changing $\phi_{PPO,\lambda}$ daily partial photo-oxidation rates differ by a factor of 1.03 ± 0.09.

Implications

Changes in DOM photo-lability have been studied in seawater from various sites with inconsistent methods, photon doses, and light sources across studies. Because of high background DIC in seawater, greater photon doses are required to produce a measurable amount of CO_2 that is detectable with infrared detection (Wang et al. 2005). With higher photon doses, studies could be missing the rapid production of CO_2 at low photon doses, as shown in the current study. To investigate CO_2 production at low photon doses, studies have sparged their water samples to reduce background DIC, however that changes the water chemistry, and thus may not produce results that are characteristic of the natural system. Andrews et al. (2000) was able to track changes in $\phi_{PO,\lambda}$ in seawater every five minutes, up to four hours in a solar simulator, however the study used pulsed polarographic oxygen sensors to track O_2 consumption, or photo-oxidation, rather than measuring

CO_2 production. In addition to requiring longer exposures times due to background DIC, light exposure times and sources, and thus photon doses, vary between studies. Furthermore, reporting light exposure times is not useful when comparing across sites and studies. Rather, what needs to be reported in time course studies are absorption coefficients and photon doses.

The current study investigated changes in freshwater DOM ϕ_λ with consistent increasing photon doses allowing for comparisons between sites, dates, and DOM chemistry. Low background DIC in Imnavait Creek, Toolik Inlet, and the Kuparuk River allowed for light exposure times as low as two hours (corresponding photon doses in Table 2), capturing the rapid production of CO_2 at low photon doses. Additionally, exposure times in this study were consistent throughout the season and by site, allowing comparisons by site and date. Imnavait Creek, Toolik Inlet, and Kuparuk River photon doses received by the water were similar, though rates of light absorption were different between sites and dates because of varying amounts of CDOM present in the waters. As mentioned in the Methods, the Sagavanirktok River water received high photon doses in this study, however the light absorbed by CDOM was not greater compared to the other three sites. Therefore, the higher photon doses received by the Sagavanirktok River water in this study are likely not causing the river's different trends in DOM lability. These controls on DOM lability with increasing photon dose have not previously been investigated in freshwaters.

Conclusions

The effect of photon dose on $\phi_{PM,350}$ and $\phi_{PPO,350}$ differ by site and date. Trends in $\phi_{PM,350}$ and $\phi_{PPO,350}$ by date are likely due to differences in initial DOM composition and source, due in part to DOM draining from deeper soils later in the season. Trends in $\phi_{PM,350}$ and $\phi_{PPO,350}$ by site are likely due to differences in DOM composition between the streams and rivers. Imnavait Creek,

Toolik Inlet, and Kuparuk River DOM composition are similar, and the Sagavanirktok River DOM is different from the other three sites. This is likely causing $\phi_{PM,350}$ and $\phi_{PPO,350}$ trends with increasing photon dose in the Sagavanirktok River because the DOM has a lower anti-oxidant capacity, relative to the three other sites in this study. The effect of changing $\phi_{PM,\lambda}$ with photon dose on the areal rates of photo-mineralization leads to an over or underestimate of photo-mineralization areal rates by a factor of 2.08 ± 0.18, calculating the areal rate with the $\phi_{PM,\lambda}$ from the shortest photon dose vs. using the $\phi_{PM,\lambda}$ from the 12-hour exposure experiment. When comparing the areal rate calculated using the 12-hour light exposure $\phi_{PM,\lambda}$ compared to the areal rate calculated with a changing $\phi_{PM,\lambda}$, photo-mineralization areal rates differ by a factor of 1.00 ± 0.11. The effect of changing $\phi_{PPO,\lambda}$ with photon dose on the areal rates of partial photo-oxidation leads to an over or underestimate of partial photo-oxidation areal rates by a factor of 1.15 ± 0.10, calculating the areal rate with the $\phi_{PPO,\lambda}$ from the shortest photon dose vs. the $\phi_{PPO,\lambda}$ from the 12-hour exposure experiment. When comparing the areal rate calculated using the 12-hour light exposure $\phi_{PPO,\lambda}$ compared to the areal rate calculated with a changing $\phi_{PPO,\lambda}$, partial photo-oxidation areal rates differ by a factor of 1.03 ± 0.09. Thus, photon dose impacts calculated areal rates of photo-mineralization and partial photo-oxidation, therefore photochemistry studies need to report photon doses received by samples to allow comparison across sites and studies.

Acknowledgements

References

Aeschbacher, M., Graf, C., Schwarzenbach, R. P., & Sander, M. (2012). Antioxidant Properties of Humic Substances. *Environmental Science & Technology*, *46*(9), 4916–4925. http://doi.org/10.1021/es300039h

Amon, R. M. W., & Benner, R. (1996). Photochemical and microbial consumption of dissolved organic carbon and dissolved oxygen in the Amazon River system. *Geochimica Et Cosmochimica Acta*, *60*(10), 1783–1792. http://doi.org/10.1016/0016-7037(96)00055-5

Andrews, S. S., Caron, S., & Zafiriou, O. C. (2000). Photochemical oxygen consumption in marine waters: A major sink for colored dissolved organic matter? *Limnology and Oceanography*, *45*(2), 267–277. http://doi.org/10.4319/lo.2000.45.2.0267

Battin, T. J., Luyssaert, S., Kaplan, L. A., Aufdenkampe, A. K., Richter, A., & Tranvik, L. J. (2009). The boundless carbon cycle. *Nature Geoscience*, *2*(9), 598–600. http://doi.org/10.1038/ngeo618

Bird, R. E., & Riordan, C. (1986). Simple solar spectral model for direct and diffuse irradiance on horizontal and tilted planes at the earth's surface for cloudless atmospheres. *Journal of Climate and Applied Meteorology*, *25*(1), 87–97. http://doi.org/10.1175/1520-0450(1986)025<0087:sssmfd>2.0.co;2

Blough N.V., Zepp R.G. (1995) Reactive Oxygen Species in Natural Waters. In: Foote C.S., Valentine J.S., Greenberg A., Liebman J.F. (eds) Active Oxygen in Chemistry. Structure Energetics and Reactivity in Chemistry Series (SEARCH Series), vol 2. Springer, Dordrecht

Carter, L. D., Heginbottom, J. A., and Woo, M.-K., 1987: Arctic lowlands. *In* Graf, W. L. (ed.), *Geomorphic Systems of North America*. Centennial Special Volume 2. Boulder, Colo.: Geological Society of America, 583-627.

Coble, P. G. (1996). Characterization of marine and terrestrial DOM in seawater using excitation-emission matrix spectroscopy. *Marine Chemistry*, *51*(4), 325–346. http://doi.org/10.1016/0304-4203(95)00062-3

Cole, J. J., Prairie, Y. T., Caraco, N. F., McDowell, W. H., Tranvik, L. J., Striegl, R. G., et al. (2007). Plumbing the Global Carbon Cycle: Integrating Inland Waters into the Terrestrial Carbon Budget. *Ecosystems*, *10*(1), 172–185. http://doi.org/10.1007/s10021-006-9013-8

Cooper, W. J., & Zika, R. G. (1983). Photochemical Formation of Hydrogen Peroxide in Surface and Ground Waters Exposed to Light. *Science*, *220*(4598), 711–712. http://doi.org/10.1126/science.220.4598.711

Cory, R. M., McKnight, D. M., Chin, Y.-P., Miller, P., & Jaros, C. L. (2007). Chemical characteristics of fulvic acids from Arctic surface waters: Microbial contributions and photochemical transformations. *Journal of Geophysical Research: Biogeosciences*, *112*(G4), G04S51. http://doi.org/10.1029/2006jg000343

Cory, R. M., McNeill, K., Cotner, J. P., Amado, A., Purcell, J. M., & Marshall, A. G. (2010a). Singlet Oxygen in the Coupled Photochemical and Biochemical Oxidation of Dissolved Organic Matter. *Environmental Science & Technology*, *44*(10), 3683–3689. http://doi.org/10.1021/es902989y

Cory, R. M., Miller, M. P., McKnight, D. M., Guerard, J. J., & Miller, P. L. (2010b). Effect of instrument-specific response on the analysis of fulvic acid fluorescence spectra. *Limnology and Oceanography: Methods*, *8*(2), 67–78. http://doi.org/10.4319/lom.2010.8.67

Cory, R. M., Crump, B. C., Dobkowski, J. A., & Kling, G. W. (2013). Surface exposure to light stimulates CO2 release from permafrost soil carbon in the Arctic. *Proceedings of the National Academy of Sciences*, *110*, 3429–3434. http://doi.org/10.1073/pnas.1214104110

Cory, R. M., Ward, C. P., Crump, B. C., & Kling, G. W. (2014). Light controls water column processing of carbon in arctic fresh waters. *Science*, *345*(6199), 925–928. http://doi.org/10.1126/science.1255006

Cory, R. M., Harrold, K. H., Neilson, B. T., & Kling, G. W. (2015). Controls on dissolved organic matter (DOM) degradation in a headwater stream: the influence of photochemical and hydrological conditions in determining light-limitation or substrate-limitation of photo-degradation. *Biogeosciences*, *12*(22), 6669–6685. http://doi.org/10.5194/bg-12-6669-2015

Farjalla, V. F., Anesio, A. M., Bertilsson, S., & Graneli, W. (2001). Photochemical reactivity of aquatic macrophyte leachates: abiotic transformations and bacterial response. *Aquatic Microbial Ecology*, *24*(2), 187–195. http://doi.org/10.3354/ame024187

Giblin, A. E., Laundre, J. A., Nadelhoffer, K. J., & Shaver, G. R. (1994). Measuring Nutrient Availability in Arctic Soils Using Ion Exchange Resins: A Field Test. *Soil Science Society of America Journal*, *58*(4), 1154–10. http://doi.org/10.2136/sssaj1994.03615995005800040021x

Hamilton, T. D., & Porter, S. C. (1975). Itkillik Glaciation in the Brooks Range, Northern Alaska. *Quaternary Research*, *5*(4), 471–497. http://doi.org/10.1016/0033-5894(75)90012-5

Hamilton, T. D.: Late Cenozoic glaciation of the central Brooks Range, in: Glaciation in Alaska-The geologic record, edited by: Hamilton, T. D., Reed, K. M., and Thorson, R. M., Alaska Geological Society, 9–50, 1986.

Helms, J. R., Stubbins, A., Ritchie, J. D., Minor, E. C., Kieber, D. J., & Mopper, K. (2008). Absorption spectral slopes and slope ratios as indicators of molecular weight, source, and photobleaching of chromophoric dissolved organic matter. *Limnology and Oceanography*, *53*(3), 955–969. http://doi.org/10.4319/lo.2008.53.3.0955

Hershey, A. E., Bowden, W. B., Deegan, L. A., & Hobbie, J. E. (1997). The Kuparuk River: a long-term study of biological and chemical processes in an arctic river. *Freshwaters of Alaska*, *119*(Chapter 4), 107–129. http://doi.org/10.1007/978-1-4612-0677-4_4

Hobara, S., Koba, K., Ae, N., Giblin, A. E., Kushida, K., & Shaver, G. R. (2013). Geochemical Influences on Solubility of Soil Organic Carbon in Arctic Tundra Ecosystems. *Soil Science Society of America Journal*, *77*(2), 473–10. http://doi.org/10.2136/sssaj2012.0199

Hu, C., Muller-Karger, F. E., & Zepp, R. G. (2002). Absorbance, absorption coefficient, and apparent quantum yield: A comment on common ambiguity in the use of these optical concepts. *Limnology and Oceanography*, *47*(4), 1261–1267. http://doi.org/10.4319/lo.2002.47.4.1261

Johannessen, S.C. and Miller, W. L. (2001). Quantum yield for the photochemical production of dissolved inorganic carbon in seawater. *Marine Chemistry*. **76**, 271–283. doi:10.1016/S0304-4203(01)00067-6

Kane, D. L., Hinzman, L. D., Benson, C. S., & Everett, K. R. (1989). Hydrology of Imnavait Creek, an arctic watershed. *Ecography*, *12*(3), 262–269. http://doi.org/10.1111/j.1600-0587.1989.tb00845.x

Keller, K., Blum, J. D., & Kling, G. W. (2010). Stream geochemistry as an indicator of increasing permafrost thaw depth in an arctic watershed, *273*(1-2), 76–81.

Kling, G. W., Kipphut, G. W., Miller, M. M., & O'Brien, W. J. (2000). Integration of lakes and streams in a landscape perspective: the importance of material processing on spatial patterns and temporal coherence. *Freshwater Biology*, *43*(3), 477–497. http://doi.org/10.1046/j.1365-2427.2000.00515.x

Latch, D. E., & McNeill, K. (2006). Microheterogeneity of Singlet Oxygen Distributions in Irradiated Humic Acid Solutions. *Science*, *311*(5768), 1743–1747. http://doi.org/10.1126/science.1121636

Levine, M. A., & Whalen, S. C. (2001). Nutrient limitation of phytoplankton production in Alaskan Arctic foothill lakes. *Hydrobiologia*, *455*, 189–201.

Lindell, M. J., Granéli, H. W., & Bertilsson, S. (2000). Seasonal photoreactivity of dissolved organic matter from lakes with contrasting humic content. *Canadian Journal of Fisheries and Aquatic Sciences*, *57*(5), 875–885. http://doi.org/10.1139/f00-016

McGuire, A. D., Anderson, L. G., Christensen, T. R., Dallimore, S., Guo, L., Hayes, D. J., et al. (2009). Sensitivity of the carbon cycle in the Arctic to climate change, *79*(4), 523–555. http://doi.org/10.1890/08-2025.1

McNamara, J.P. Kane, D.L. and Hinzman, L.D. (1998). An analysis of streamflow hydrology in the Kuparuk River Basin, Arctic Alaska: a nested watershed approach. *Journal of Hydrology 206*, 39-57.

McNamara, J.P., Kane, D.L., Hobbie, J.E., and Kling, G.W. (2008). Hydrologic and biogeochemical controls on the spatial and temporal patterns of nitrogen and phosphorus in the Kuparuk River, arctic Alaska. *Hydrological Processes 22*(17): 3294-3309.

Miles, C. J., & Brezonik, P. L. (1981). Oxygen consumption in humic-colored waters by a photochemical ferrous-ferric catalytic cycle. *Environmental Science & Technology*, *15*(9), 1089–1095. http://doi.org/10.1021/es00091a010

Miller, W. L., & Zepp, R. G. (1995). Photochemical production of dissolved inorganic carbon from terrestrial organic matter: Significance to the oceanic organic carbon cycle. *Geophysical Research Letters*, *22*(4), 417–420. http://doi.org/10.1029/94GL03344

Mopper, K., & Zhou, X. (1990). Hydroxyl Radical Photoproduction in the Sea and Its Potential Impact on Marine Processes. *Science*, *250*(4981), 661–664. http://doi.org/10.1126/science.250.4981.661

Olefeldt, D., & Roulet, N. T. (2012). Effects of permafrost and hydrology on the composition and transport of dissolved organic carbon in a subarctic peatland complex. *Journal of Geophysical Research: Biogeosciences*, *117*(G1). http://doi.org/10.1029/2011jg001819

Osterkamp, T. E. and Payne, M. W. (1981). Estimates of permafrost thick- ness from well logs in northern Alaska, *Cold Regions Science and Technology*, *5*, 13–27.

Page, S. E., Logan, J. R., Cory, R. M., & McNeill, K. (2014). Evidence for dissolved organic matter as the primary source and sink of photochemically produced hydroxyl radical in arctic surface waters. *Environmental Sciences: Processes & Impacts*, *16*(4), 807. http://doi.org/10.1039/c3em00596h

Poulin, B. A., Ryan, J. N., & Aiken, G. R. (2014). Effects of Iron on Optical Properties of Dissolved Organic Matter. *Environmental Science & Technology*, *48*(17), 10098–10106. http://doi.org/10.1021/es502670r

Powers, L. C., & Miller, W. L. (2015a). Photochemical production of CO and CO2 in the Northern Gulf of Mexico: Estimates and challenges for quantifying the impact of photochemistry on carbon cycles. *Marine Chemistry*, *171*(C), 21–35. http://doi.org/10.1016/j.marchem.2015.02.004

Powers, L. C., & Miller, W. L. (2015b). Hydrogen peroxide and superoxide photoproduction in diverse marine waters: A simple proxy for estimating direct CO2 photochemical fluxes, 1–9. http://doi.org/10.1002/(ISSN)1944-8007

Pullin, M. J., Bertilsson, S., Goldstone, J. V., & Voelker, B. M. (2004). Effects of light and hydroxyl radical on dissolved organic matter: Bacterial growth efficiency and production of carboxylic acids and other substrates. *Limnology and Oceanography*, *49*(6), 2011–2022. http://doi.org/10.4319/lo.2004.49.6.2011

Rember, R. D., & Trefry, J. H. (2004). Increased concentrations of dissolved trace metals and organic carbon during snowmelt in rivers of the alaskan arctic. *Geochimica Et Cosmochimica Acta*, *68*(3), 477–489. http://doi.org/10.1016/S0016-7037(03)00458-7

Schwarzenbach, R. P.; Gschwend, P. M.; Imboden, D. M. Environmental Organic Chemistry, 2nd ed.; Wiley: New York, 2003.

Sharpless, C. M., Aeschbacher, M., Page, S. E., Wenk, J., Sander, M., & McNeill, K. (2014). Photooxidation-Induced Changes in Optical, Electrochemical, and Photochemical Properties of Humic Substances. *Environmental Science & Technology*, *48*(5), 2688–2696. http://doi.org/10.1021/es403925g

Tarnocai, C., Canadell, J. G., Schuur, E. A. G., Kuhry, P., Mazhitova, G., & Zimov, S. (2009). Soil organic carbon pools in the northern circumpolar permafrost region. *Global Biogeochemical Cycles*, *23*(2), n/a–n/a. http://doi.org/10.1029/2008GB003327

Townsend-Small, A., McClelland, J. W., Holmes, R. M., & Peterson, B. J. (2010). Seasonal and

hydrologic drivers of dissolved organic matter and nutrients in the upper Kuparuk River, Alaskan Arctic. *Biogeochemistry*, *103*(1-3), 109–124. http://doi.org/10.1007/s10533-010-9451-4

Vähatalo, A. V. V. Ä., Salonen, M. S., Taalas, P., & Salonen, K. (2000). Spectrum of the quantum yield for photochemical mineralization of dissolved organic carbon in a humic lake. *Limnology and Oceanography*, *45*(3), 664–676. http://doi.org/10.4319/lo.2000.45.3.0664

Wang, Z.A., Cai, W.-J., Wang, Y., & Ji, H. (2005). The southeastern continental shelf of the United States as an atmospheric CO2 source and an exporter of inorganic carbon to the ocean. *Continental Shelf Research*, *25*(16), 1917–1941. http://doi.org/10.1016/j.csr.2005.04.004

Ward, C. P., & Cory, R. M. (2015). Chemical composition of dissolved organic matter draining permafrost soils. *Geochimica Et Cosmochimica Acta*, *167*, 63–79. http://doi.org/10.1016/j.gca.2015.07.001

Ward, C. P., & Cory, R. M. (2016). Complete and Partial Photo-oxidation of Dissolved Organic Matter Draining Permafrost Soils. *Environmental Science & Technology*, *50*(7), 3545–3553. http://doi.org/10.1021/acs.est.5b05354

Weishaar, J. L.; Aiken, G. R.; Bergamaschi, B. A.; Fram, M. S.; Fujii, R.; Mopper, K. Evaluation of specific ultraviolet absorbance as an indicator of the chemical composition and reactivity of dissolved organic carbon. Environ. Sci. Technol. 2003, 37, 4702−4708.

Wetzel, R. G., Hatcher, P. G., & Bianchi, T. S. (1995). Natural photolysis by ultraviolet irradiance of recalcitrant dissolved organic matter to simple substrates for rapid bacterial metabolism. *Limnology and Oceanography*, *40*(8), 1369–1380. http://doi.org/10.4319/lo.1995.40.8.1369

Wetzel, R. G.: Lake and River Ecosystems, Limnology, 37, 490– 525, 2001.

Zhang, Y., Chen, W., & Riseborough, D. W. (2006). Temporal and spatial changes of permafrost in Canada since the end of the Little Ice Age. *Journal of Geophysical Research: Biogeosciences*, *111*(D22), 157–14. http://doi.org/10.1029/2006JD007284

Tables and Figures

	Imnavait Creek	Toolik Inlet	Kuparuk River	Sagavanirktok River
Latitude (°N)	68°37'	68°38'	68°39'	68°48'
Longitude (°W)	149°19'	149°36'	149°25'	148°51'
n	65	85	9	5
Temperature (°C)	9.2 ± 5.8	9.0 ± 4.6	4.8 ± 4.3	5.5 ± 5.4
pH	5.6 ± 0.5	7.3 ± 0.3	7.0 ± 0.6	7.6 ± 0.6
Conductivity (μS cm^{-1})	11.7 ± 3.9	86.1 ± 21.5	43.9 ± 24.5	198 ± 35.7
a305 (m^{-1}) [a]	59.0 ± 9.2	20.1 ± 8.3	32.7 ± 17.6	12.5 ± 7.7

[a]a305 is the absorbance at 305 nm of 0.7 μm filtered surface water.

Table 1. Characteristics of study sites in May – August of 2016 and 2017. Shown are the mean ± standard error.

| Site/Date	Hours of sunlight exposure	Photon Dose (mol photons m^{-2})
Imnavait Creek		
19-May-2017	2, 4, 8, 12, 16	10, 20, 41, 63, 83
5-July-2017	2, 4, 8, 12, 16	10, 20, 29, 50, 59
27-July-2017	2, 4, 8, 12, 18	7, 15, 23, 36, 63
Toolik Inlet		
19-May-2017	2, 4, 8, 12, 16	10, 21, 33, 51, 72
21-July-2017	3, 7, 12, 19, 24	11, 23, 32, 43, 55
Kuparuk River		
25-May-2017	2, 4, 8, 12, 16	10, 20, 41, 63, 83
4-July-2017	2, 4, 8, 12, 16	9, 17, 31, 51, 60
27-July-2017	2, 4, 8, 12, 16	9, 18, 30, 47, 65
Sagavanirktok River		
5-June-2017	4, 8, 12, 18, 24	26, 43, 63, 91, 121
17-July-2017	2, 4, 8, 12, 19, 28	8, 16, 24, 37, 56, 59

Table 2. Hours of light exposure and corresponding photon doses received in each experiment.

Site/Date	Temperature °C	pH ± 0.1	Conductivity μs cm^{-1}	a305 m^{-1}	DOC μM	SUVA$_{254}$ L mg C^{-1} m^{-1}	SR	FI	E2/E3
Imnavait Creek									
19-May-2017	0.1	4.8	13	63 ± 0.04	1371	3.3	0.74 ± 0.001	1.49 ± 0.003	5.02 ± 0.003
5-July-2017	16	5.9	12	46 ± 0.04	888	3.9	0.79 ± 0.001	1.47 ± 0.003	5.05 ± 0.003
27-July-2017	10	5.7	11	54 ± 0.04	1105	3.6	0.76 ± 0.001	1.53 ± 0.004	5.47 ± 0.01
Toolik Inlet									
19-May-2017	0.1	7.6	92	29 ± 0.02	693	3.1	0.87 ± 0.001	1.54 ± 0.005	4.93 ± 0.01
21-July-2017	12	7.3	85	15 ± 0.04	418	2.8	0.90 ± 0.004	1.58 ± 0.003	5.99 ± 0.04
Kuparuk									
25-May-2017	0.1	6.7	18	53 ± 0.06	1006	3.5	0.76 ± 0.001	1.47 ± 0.003	4.51 ± 0.01
4-July-2017	10	7.8	77	6 ± 0.02	170	2.6	1.00 ± 0.01	1.54 ± 0.006	5.77 ± 0.05
27-July-2017	7	7.4	63	17 ± 0.06	408	3.1	0.81 ± 0.003	1.56 ± 0.003	5.30 ± 0.05
Sagavanirktok									
5-June-2017	5	7.8	189	6 ± 0.03	142	3.2	1.01 ± 0.013	1.50 ± 0.004	5.34 ± 0.04
17-July-2017	11	8.1	245	3 ± 0.02	99	2.8	0.91 ± 0.006	1.63 ± 0.004	5.13 ± 0.30

Table 3. Initial water and DOM chemistry of surfaces waters in this study. Shown are the mean ± standard error.
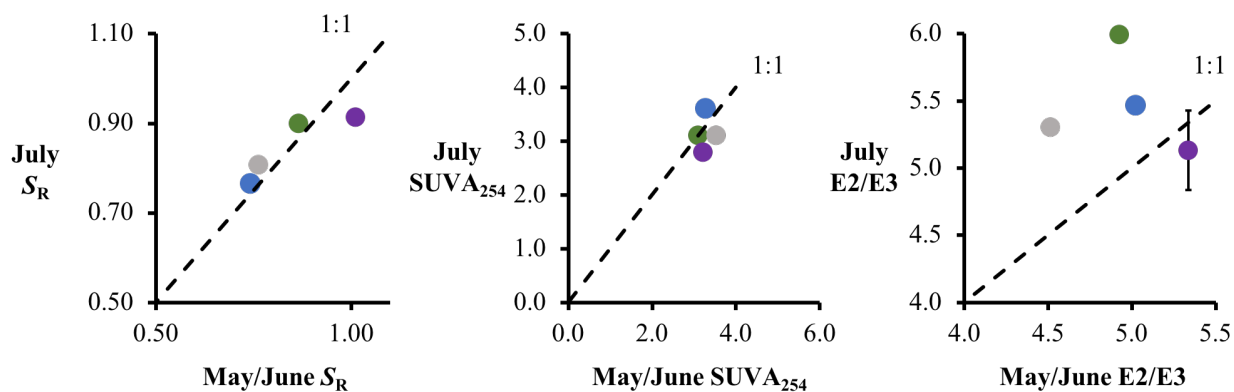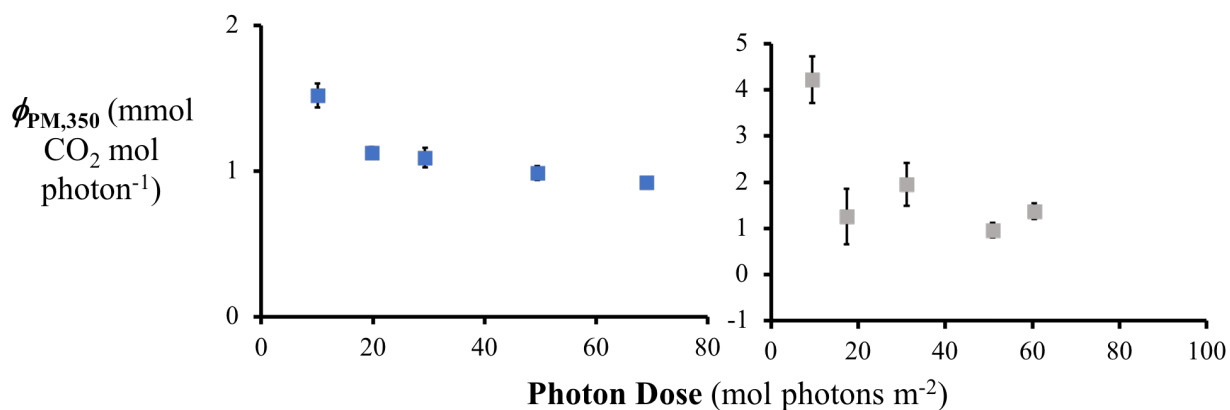

Figure 1. Comparison of CDOM chemistry proxies in May/June (x-axis) vs. July (y-axis) in Imnavait Creek (blue), Toolik Inlet (green), the Kuparuk River (grey), and the Sagavanirktok River (purple). Shown are the mean ± standard error.
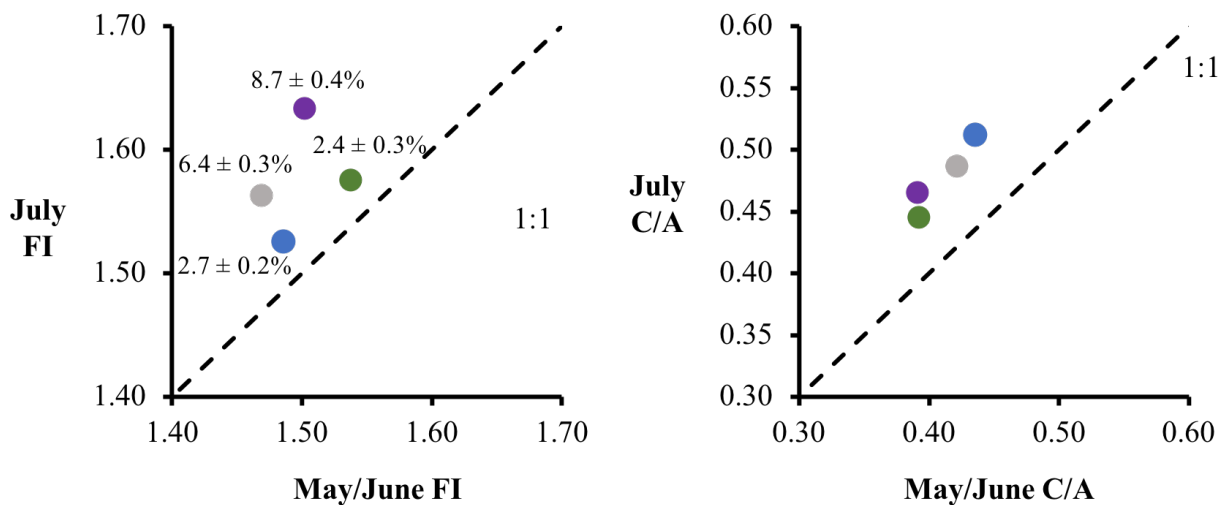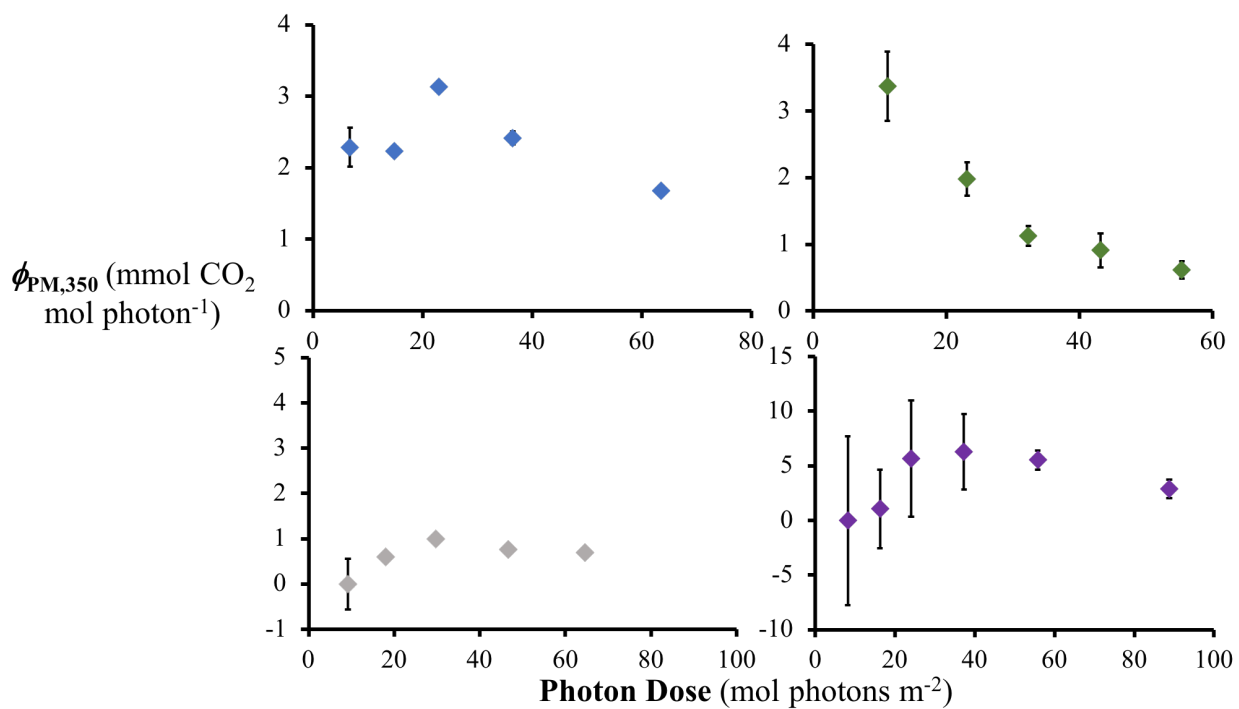
Figure 2. Comparison of FDOM chemistry proxies in May/June (x-axis) vs. July (y-axis) in Imnavait Creek (blue), Toolik Inlet (green), the Kuparuk River (grey), and the Sagavanirktok River (purple). Percentages shown on the FI plot are % change in FI between May/June and July. Shown are the mean ± standard error.
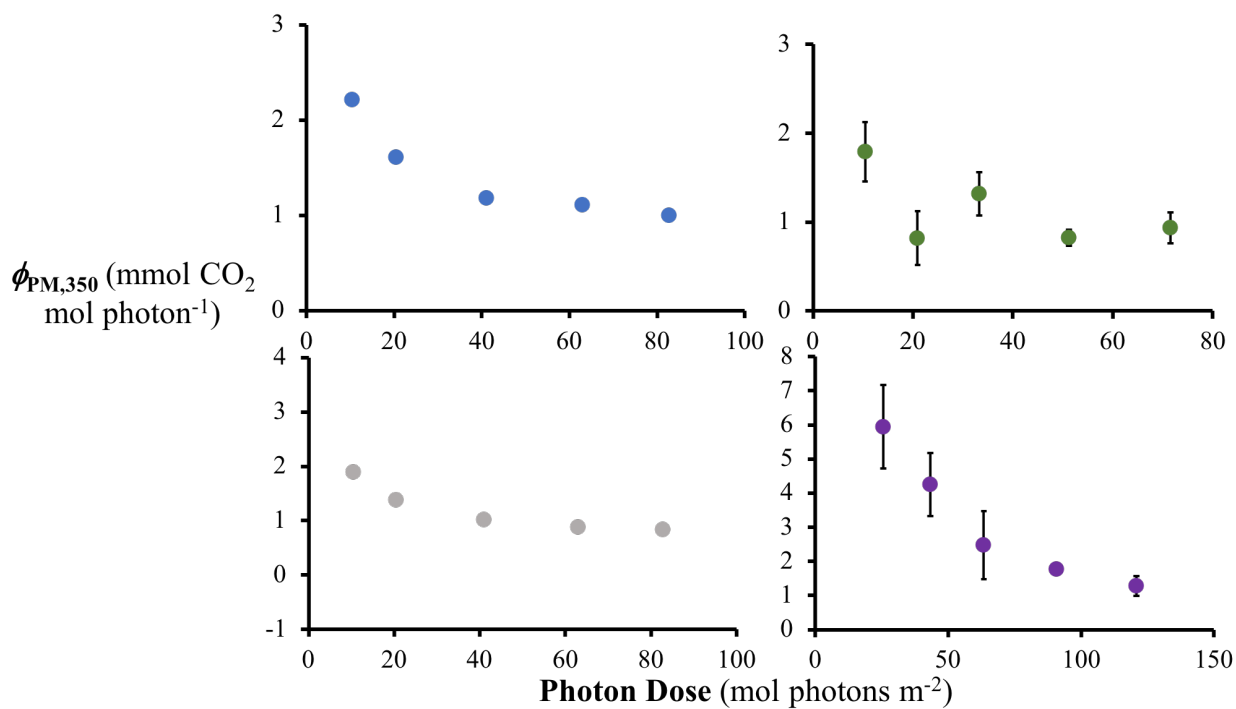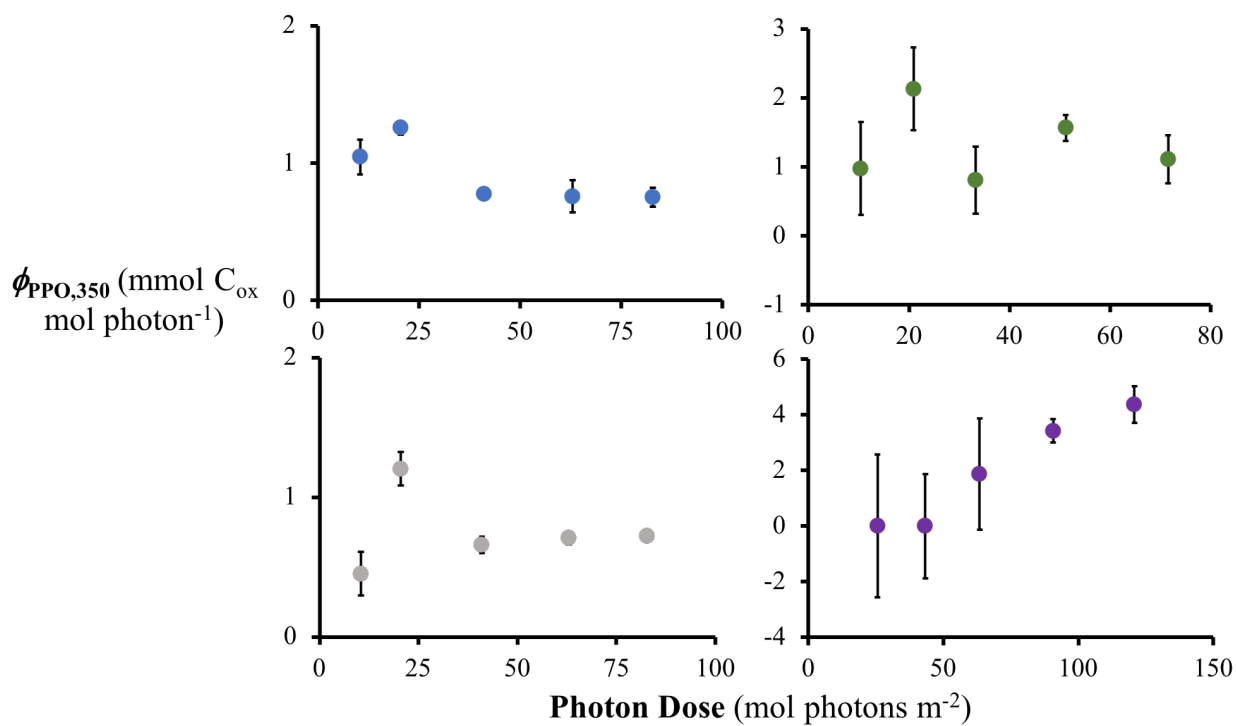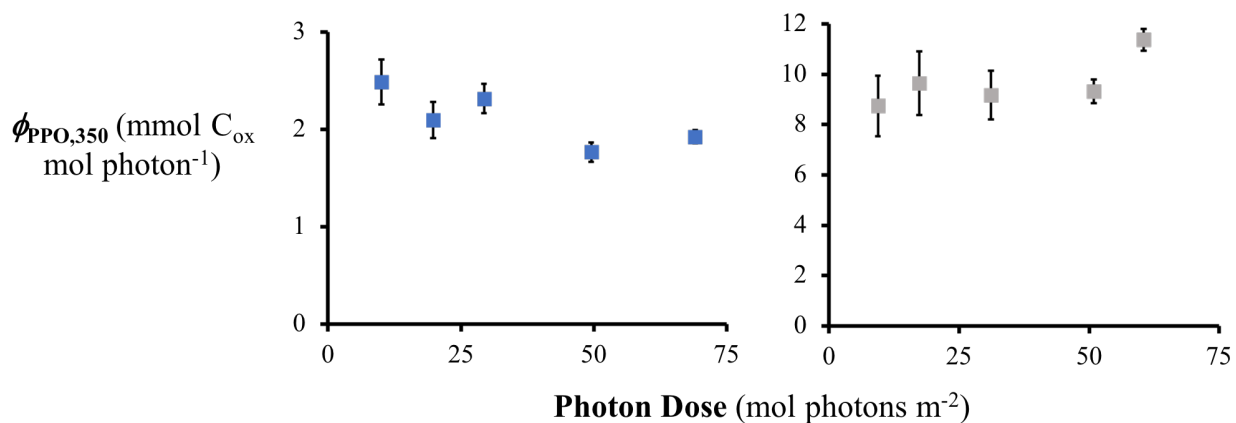
Figure 3. May/June $\phi_{PM,350}$ (y-axis) with increasing photon dose (x-axis) in Imnavait Creek (blue), Toolik Inlet (green), the Kuparuk River (grey), and the Sagavanirktok River (purple). Shown are the mean ± standard error.

Figure 4. Early July $\phi_{PM,350}$ (y-axis) with increasing photon dose (x-axis) in Imnavait Creek (blue) and the Kuparuk River (grey), which were the only waters tested on this date. Shown are the mean ± standard error.
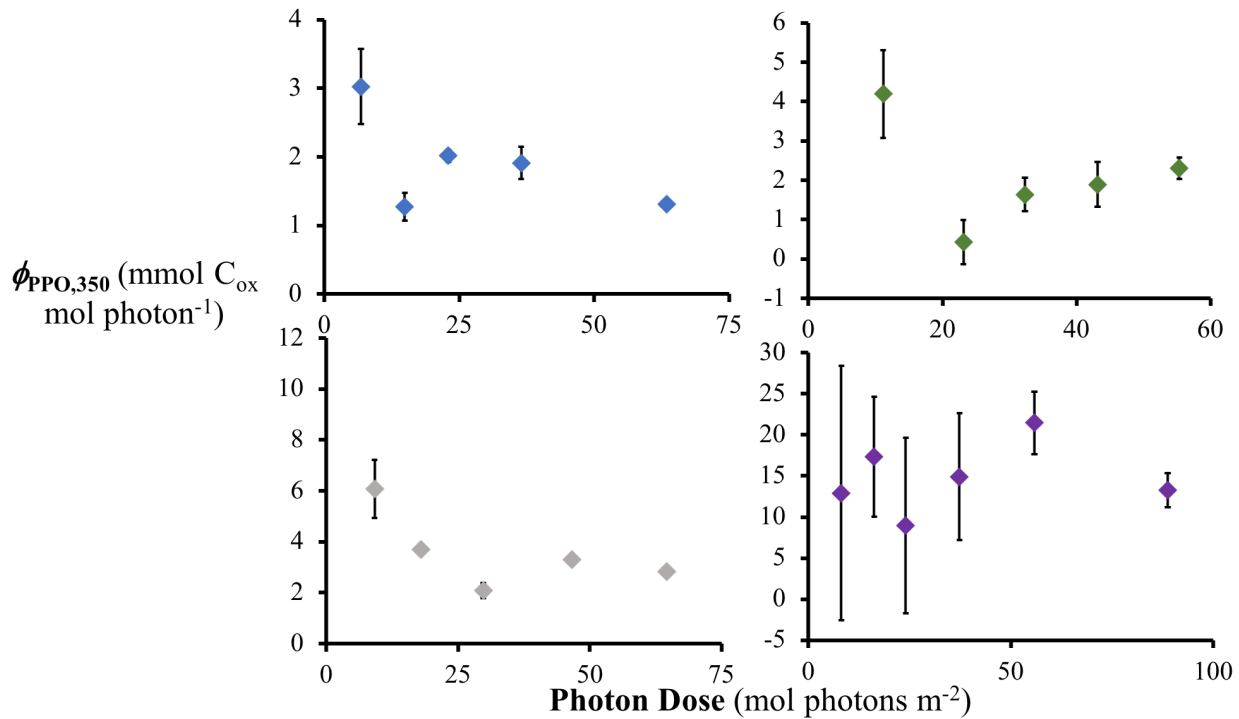
Figure 5. Late July $\phi_{PM,350}$ (y-axis) with increasing photon dose (x-axis) in Imnavait Creek (blue), Toolik Inlet (green), the Kuparuk River (grey), and the Sagavanirktok River (purple). Shown are the mean ± standard error.
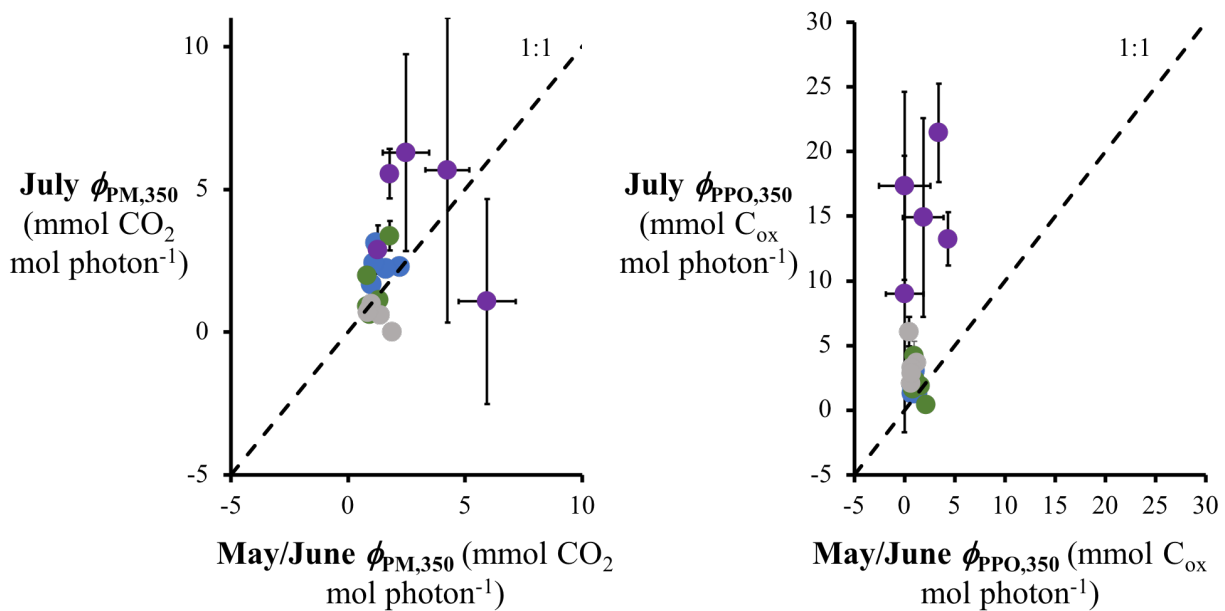
Figure 6. May/June $\phi_{PPO,350}$ (y-axis) with increasing photon dose (x-axis) in Imnavait Creek (blue), Toolik Inlet (green), the Kuparuk River (grey), and the Sagavanirktok River (purple). Shown are the mean ± standard error.

Figure 7. Early July $\phi_{PPO,350}$ (y-axis) with increasing photon dose (x-axis) in Imnavait Creek (blue) and the Kuparuk River (grey), which were the only waters tested on this date. Shown are the mean ± standard error.
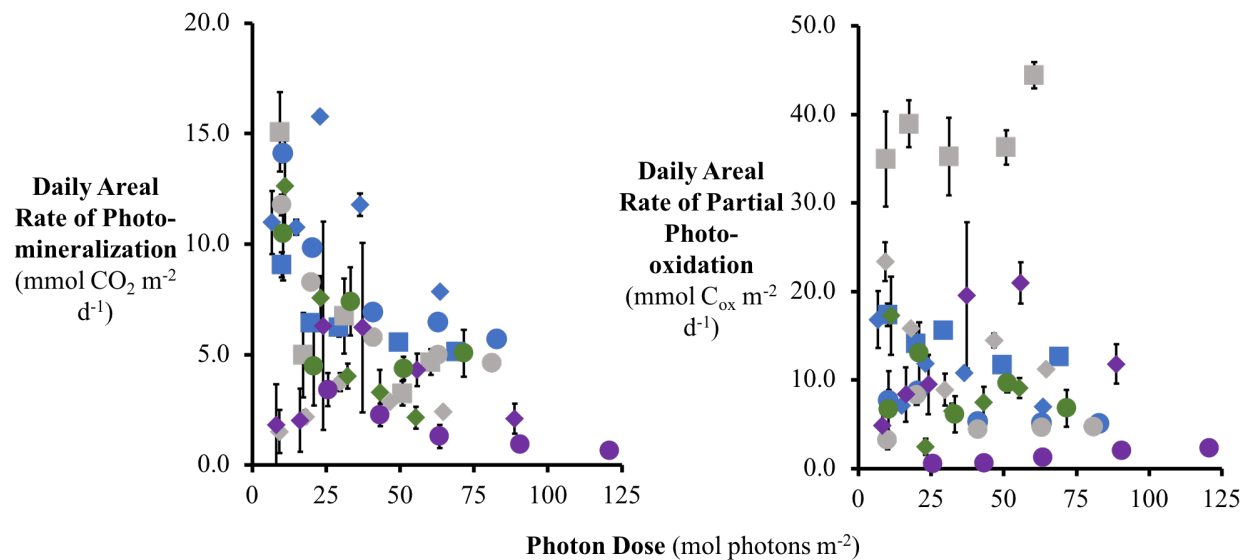
Figure 8. Late July $\phi_{PPO,350}$ (y-axis) with increasing photon dose (x-axis) in Imnavait Creek (blue), Toolik Inlet (green), the Kuparuk River (grey), and the Sagavanirktok River (purple). Shown are the mean ± standard error.
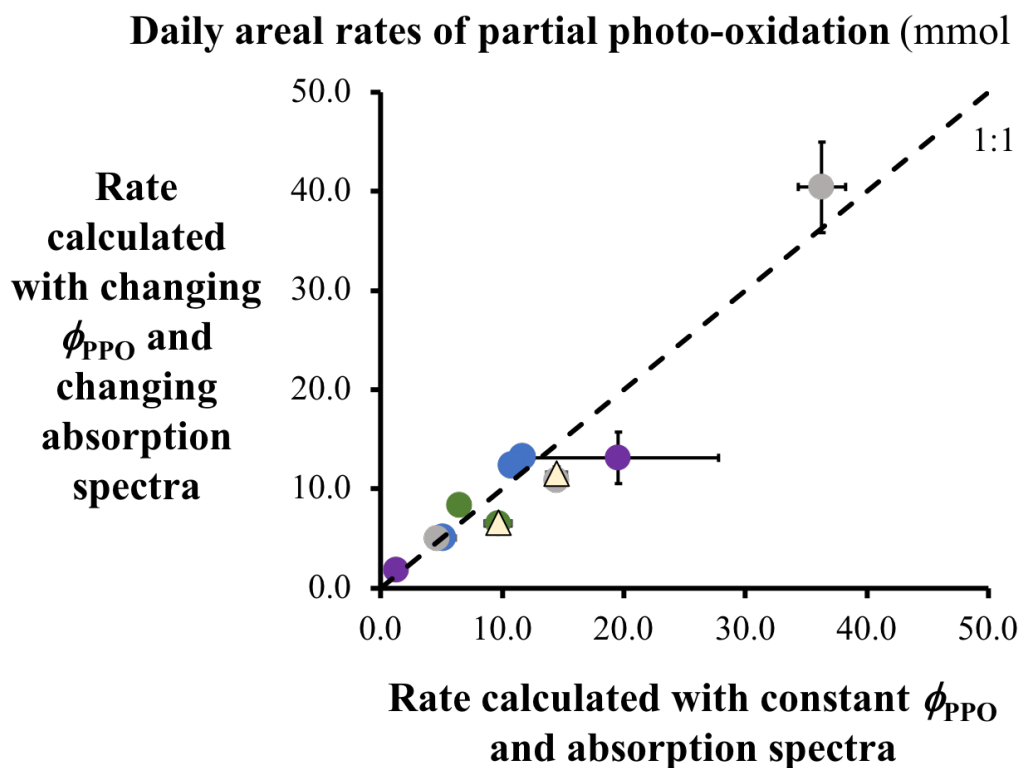
Figure 9. Comparison of (a) $\phi_{PM,350}$ and (b) $\phi_{PPO,350}$ in May/June (x-axis) vs. July (y-axis) in Imnavait Creek (blue), Toolik Inlet (green), the Kuparuk River (grey), and the Sagavanirktok River (purple). Shown are the mean ± standard error.

Figure 10. Daily areal rates of (a) photo-mineralization and (b) partial photo-oxidation (y-axes) calculated with (a) $\phi_{PM,350}$ and (b) $\phi_{PPO,350}$ corresponding to the cumulative photon dose (x-axes) of that light exposure increment in Imnavait Creek (blue), Toolik Inlet (green), the Kuparuk River (grey), and the Sagavanirktok River (purple). Collection date is indicated by May/June (circle), early July (square), and late July (diamond). Shown are the mean ± standard error.

Daily areal rates of photo-mineralization (mmol CO_2 m^{-2} d^{-1})
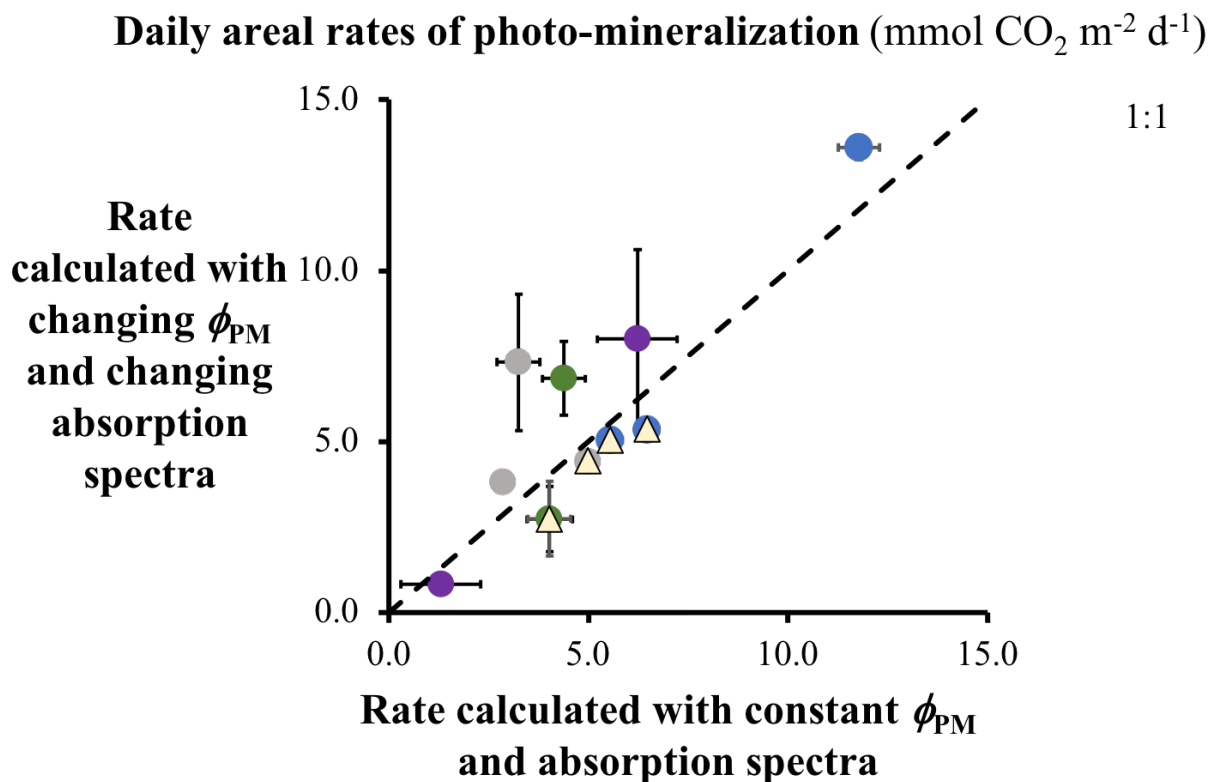
Figure 11. Comparison of daily areal rates of photo-mineralization calculated with a constant $\phi_{PM,350}$ and absorption spectra (x-axis) vs. a changing $\phi_{PM,350}$ and absorption spectra (y-axis) in Imnavait Creek (blue), Toolik Inlet (green), the Kuparuk River (grey), and the Sagavanirktok River (purple). Triangles represent the rate calculated with changing $\phi_{PM,350}$ and a constant absorption spectrum, showing that photobleaching was not causing these points to fall below the 1:1 line. Shown are the mean ± standard error.

Daily areal rates of partial photo-oxidation (mmol C_{ox} m^{-2} d^{-1})

Figure 12. Comparison of daily areal rates of photo-mineralization calculated with a constant $\phi_{PPO,350}$ and absorption spectra (x-axis) vs. a changing $\phi_{PPO,350}$ and absorption spectra (y-axis) in Imnavait Creek (blue), Toolik Inlet (green), the Kuparuk River (grey), and the Sagavanirktok River (purple). Triangles represent the rate calculated with changing $\phi_{PPO,350}$ and a constant absorption spectrum, showing that photobleaching was not causing these points to fall below the 1:1 line. Shown are the mean ± standard error.